Proc. Natl. Acad. Sci. USA
Vol. 91, pp. 5617–5621, June 1994
Biophysics

Proton conduction within the reaction centers of *Rhodobacter capsulatus*: The electrostatic role of the protein

(photochemical reaction center/proton transfer/electron transfer/site-specific mutagenesis)

PÉTER MARÓTI*†, DEBORAH K. HANSON§, LAURA BACIOU*¶, MARIANNE SCHIFFER§, AND PIERRE SEBBAN*||

*Photosynthèse Bactérienne, Centre de Génétique Moléculaire, Bât. 24, Centre National de la Recherche Scientifique, 91198, Gif/Yvette, France; and §Center for Mechanistic Biology and Biotechnology, Argonne National Laboratory, 9700 South Cass Avenue, Argonne, IL 60439

Communicated by Pierre Joliot, February 28, 1994

ABSTRACT **Light-induced charge separation in the photosynthetic reaction center results in delivery of two electrons and two protons to the terminal quinone acceptor Q_B. In this paper, we have used flash-induced absorbance spectroscopy to study three strains that share identical amino acid sequences in the Q_B binding site, all of which lack the protonatable amino acids Glu-L212 and Asp-L213. These strains are the photosynthetically incompetent site-specific mutant Glu-L212/Asp-L213 → Ala-L212/Ala-L213 and two different photocompetent derivatives that carry both alanine substitutions and an intergenic suppressor mutation located far from Q_B (class 3 strain, Ala-Ala + Arg-M231 → Leu; class 4 strain, Ala-Ala + Asn-M43 → Asp). At pH 8 in the double mutant, we observe a concomitant decrease of nearly 4 orders of magnitude in the rate constants of second electron and proton transfer to Q_B compared to the wild type. Surprisingly, these rates are increased to about the same extent in both types of suppressor strains but remain >2 orders of magnitude smaller than those of the wild type. In the double mutant, at pH 8, the loss of Asp-L213 and Glu-L212 leads to a substantial stabilization (≥60 meV) of the semiquinone energy level. Both types of compensatory mutations partially restore, to nearly the same level, the original free energy difference for electron transfer from primary quinone Q_A to Q_B. The pH dependence of the electron and proton transfer processes in the double-mutant and the suppressor strains suggests that when reaction centers of the double mutant are shifted to lower pH (1.5–2 units), they function like those of the suppressor strains at physiological pH. Our data suggest that the main effect of the compensatory mutations is to partially restore the negative electrostatic environment of Q_B and to increase an apparent "functional" pK of the system for efficient proton transfer to the active site. This emphasizes the role of the protein in tuning the electrostatic environment of its cofactors and highlights the possible long-range electrostatic effects.**

Photosynthetic organisms convert light excitation energy into chemical free energy. This is accomplished at the level of the photochemical reaction centers (RCs), which span the photosynthetic membranes. The RC from the purple bacterium *Rhodopseudomonas viridis* was the first membrane protein for which successful crystallization has led to the determination of its three-dimensional structure (1). The RC structure from *Rhodobacter (Rb.) sphaeroides* was more recently determined (2–4). These complexes are constituted by three proteins, L, M, and H, whose molecular masses range between 30 and 35 kDa. The cofactors involved in the primary electron transfer processes are noncovalently bound to the L and M proteins. A transmembrane charge separation is initiated between a primary electron donor, P (situated near the periplasmic side of the membrane), and a system of two quinones, Q_A and Q_B, located near the cytoplasmic side of the membrane. Q_A, which is a one-electron acceptor, is found in a relatively hydrophobic environment of the M protein, at variance to Q_B, which functions as a two-electron acceptor and is bound in a more polar region of the L protein. Absorption of two photons by the system results in the transfer of two electrons to Q_B, the uptake of two protons by the protein, and the formation of the quinol molecule Q_BH_2. This loosely bound species leaves the RC and is replaced by an oxidized quinone from the pool present in the membrane, following which electron and proton transfers may be reinitiated.

The direct involvement of a few amino acids near Q_B in proton donation to Q_B^{2-} has recently been suggested. This was shown by studies of site-specific mutants, which were impaired or restricted in proton conduction to Q_B^{2-} (5–10). Asp-L213 (5, 6) and Ser-L223 (7) have been proposed to be involved in the donation of the first proton to Q_B, and Glu-L212 has been proposed to be involved in the donation of the second proton (6, 8, 9). In addition, it has been suggested that water molecules could participate in this process (10–12).

In the present paper, we analyze the coupling between electron and proton transfer processes in RCs from wild-type *Rb. capsulatus*, from a nonphotosynthetic (PS^-) site-specific mutant that carries substitutions at two of the above sites (Glu-L212/Asp-L213 → Ala-L212/Ala-L213), and from two different photocompetent (PS^+) derivatives isolated from this mutant. These derivatives are actually pseudorevertants, since each has retained both alanine substitutions in the Q_B binding site yet has recovered the photosynthetic phenotype as a result of a third mutation that serves as an intergenic suppressor [class 3 strain, Glu-L212/Asp-L213/Arg-M231 → Ala-L212/Ala-L213/Leu-231 (10, 13); class 4 strain, Glu-L212/Asp-L213/Asn-M43 → Ala-L212/Ala-L213/Asp-M43 (13, 14)]. These compensatory mutations lie well outside the Q_B binding pocket, and each restores one of the two negative charges eliminated by the site-specific mutations. In the wild-type *Rb. sphaeroides* RC structure, Arg-M231 is involved in conserved ion pair interactions with two residues in the H chain, Glu-H125 and Glu-H232, in a region that is 15–20 Å from Q_B. Asn-M43, 9 Å from Q_B, is part of the second layer of residues that surrounds the quinone and is located at an interface between the L, M, and H chains.

To understand the way that protons are driven to Q_B in the suppressor strains, which have the same configuration of amino acids in the Q_B binding site as the PS^- double mutant,

The publication costs of this article were defrayed in part by page charge payment. This article must therefore be hereby marked "*advertisement*" in accordance with 18 U.S.C. §1734 solely to indicate this fact.

Abbreviations: RC, reaction center; Q_A and Q_B, primary and secondary quinones; P, primary electron donor; PS^-, nonphotosynthetic; PS^+, photocompetent.

†Present address: Institute of Biophysics, József Attila University, Egyetem utca 2, Szeged, Hungary.
¶Present address: Max-Planck-Institut für Biophysik, Frankfurt, Germany.
||To whom reprint requests should be addressed.

we have studied the electrostatic influences of these mutations on the energetics of the quinone system and have analyzed the coupling between the kinetics of electron transfer to Q_B^- and proton transfer to Q_B^{2-} in the different strains.

MATERIALS AND METHODS

The construction of the Ala-L212/Ala-L213 double mutant by site-specific mutagenesis and the isolation and genetic characterization of the class 3 and class 4 suppressor strains have been described (14). Large-scale cultures for RC preparation were grown under chemoheterotrophic conditions (semiaerobic, dark, 34°C) on RPYE medium containing kanamycin to ensure the presence of the plasmid. RCs of the double-mutant and the suppressor strains were prepared as described for the wild type (15). Occupancy of the Q_B site was routinely restored by the addition of 50–100 μM coenzyme Q_6.

All experiments were carried out at 21°C on a home-made spectrophotometer (15). To avoid the presence of the stable PQ_B^- state in the double mutant before the flashes, a long (≈1 h) dark-adaptation period was imposed on the sample. Depending on the pH range, the pH buffer used in the charge recombination and second electron transfer experiments was Mes [2-(*N*-morpholino)ethanesulfonic acid], Bistris propane [bis(2-hydroxyethyl)amino]tris(hydroxymethyl) propane], or CAPS [3-(cyclohexylamino)-1-propanesulfonic acid]. Proton transfer kinetics were measured with pH indicator dyes; 40 μM cresol red, phenol red, bromocresol purple, and/or chlorophenol red was used depending on pH. The absorbance changes of the dyes were measured at 557 nm for phenol red and at 582 nm for other dyes. For the temperature dependence measurements, the temperature was monitored by using a NiCr–Ni thermocouple with a precision of ±0.3°C.

RESULTS

Semiquinone Oscillations and Cytochrome Oxidation Turnover. *The double mutant.* The cycling of Q_B through the Q_B^- and Q_B^{2-} states with successive flashes can be followed by monitoring the formation and disappearance of the semiquinone anion at 450 nm in the presence of exogenous donors to P^+ (16, 17) (see Fig. 1*A* for wild type). The oscillations in double-mutant RCs are displayed in Fig. 1*B*, measured at pH 7.8 and pH 6.2. The time spacing used in these experiments was 1 s. At pH 7.8, a complete absence of oscillations is noted. A stable Q_B^- state is formed after the first flash as in the wild type. However, a slow decay of the semiquinone signal is observed after each subsequent flash. The decay of the semiquinone signal after the second flash is attributed to the disappearance of Q_A^- and Q_B^-. The electron transfer from Q_A^- to Q_B^- is coupled to the uptake of the second proton. At pH 6.2, however, some Q_B^{2-} is formed in the double mutant, as shown by the partial recovery of semiquinone oscillations. Thus, the observed slow decay of the semiquinone signal after even flashes is limited by the slow delivery of protons in the double mutant. This is in agreement with our earlier observations (10, 13). The absence of oscillations at pH 7.8 does not arise from a poor binding of Q_B in this mutant. At this pH, occupancy of the Q_B site is 80%, as determined by measuring the relative amount of the slow phase of charge recombination reflecting the $P^+Q_B^-$ contribution to the total P^+ decay.

To better understand the reasons for electron and proton transfer deficiency in the double mutant, we have varied the flash repetition frequency in multiflash cytochrome oxidation experiments at 550 nm (Fig. 2). The ratio of the absorbance change due to oxidation of cytochrome *c* after the third flash to that after the first one ($\Delta A_3/\Delta A_1$) reflects the ability of the RCs to turn over—i.e., the ability of Q_B to accept two protons and two electrons within a certain period of time. Clearly, at pH 8, the $\Delta A3/\Delta A_1$ ratio is much smaller than 1 if the time delay between two flashes is smaller than ≈2.5 s. However, when the flash repetition frequency becomes smaller than ≈0.2 Hz, the cytochrome oxidation pattern tends not to be damped ($\Delta A_3/\Delta A_1$ approaches I at 0.1 Hz). This shows that protons may be delivered via an alternative pathway to the active site with rates that are much slower than the wild-type pathway. At pH 6.2, the points describing the $\Delta A_3/\Delta A_1$ ratio are predictably shifted to much higher frequencies, reflecting faster second electron transfer at this pH. As previously observed in *Rb. sphaeroides* (18), sodium azide helps deliver protons to the active site in the double mutant. Cytochrome turnover is recovered at pH 8 ($\Delta A_3/\Delta A_1 \approx 0.9$) in the presence of 0.7 M sodium azide, whatever the flash repetition frequency (data not shown).

The suppressor strains. The semiquinone oscillation patterns in the RCs from the class 4 strain are displayed in Fig. 1*C*. The function that is lost in the PS^- double mutant at pH 7.8 is recovered in this PS^+ strain, even though the second electron transfer step displays very slow kinetics. We have demonstrated semiquinone oscillations in RCs from the class 3 strain at the same pH (10). Faster second electron transfer was displayed in class 3 RCs (confirmed below by direct measurements), leading to somewhat less damped oscillations (10) than in the class 4 strain at pH 7.8. As was seen for the double mutant (Fig. 1*B*), lowering the pH to 6.2 in class 4 RCs substantially accelerates the protonation phenomena (Fig. 1*C*). To further understand these phenomena, we have measured the second electron and proton transfer rates in all of these strains.

Second Electron and Proton Transfer Rates. No large change in the rates of first electron transfer, measured in chromatophores, was observed in the suppressor strains compared to the wild type (13), reflecting that no net protonation of the quinone acceptor is required for the first

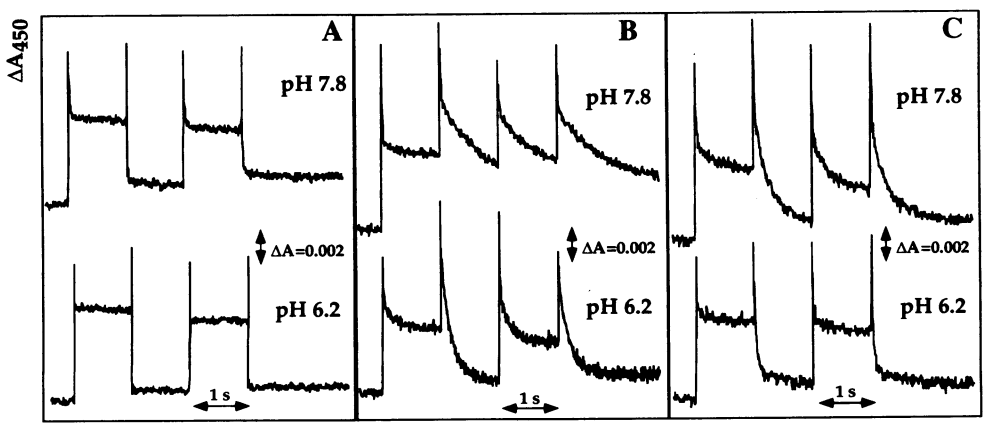

FIG. 1. Semiquinone oscillations measured at 450 nm in RCs (1.3 μM) from *Rb. capsulatus* at pH 7.8 and pH 6.2 in wild type (*A*), in the PS^- Ala-L212/Ala-L213 double mutant (*B*), and in the PS^+ class 4 suppressor strain (Ala-L212/Ala-L213 + Asn-M43 → Asp) (*C*). Conditions were 10 mM Tris (pH 7.8) or 10 mM Mes (pH 6.2), 0.05% lauryldimethylamine-*N*-oxide, 50 μM coenzyme Q_6, and 100 μM ferrocene.

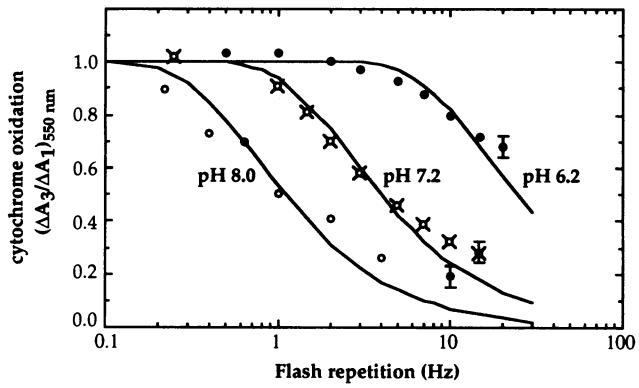

FIG. 2. Effect of flash repetition on the oxidation of cytochrome *c* turnover in the PS⁻ Ala-L212/Ala-L213 double-mutant RCs (≈1 μM), measured by the ratio of the absorbance change at 550 nm after the third flash (ΔA_3) to that after the first flash (ΔA_1). Conditions were 20 μM cytochrome *c*, 50 μM coenzyme Q_6, 500 μM ascorbic acid, 5 mM Tris (pH 7.2 and pH 8.0), and Mes (pH 6.2). Lines are drawn according to a simple model: $\Delta A_3/\Delta A_1 = 1 - e^{(k_{AB}(2)/f)}$, where *f* is the flash repetition frequency. At pH 6.2, 7.2, and 8.0, $k_{AB}(2)$ values were taken as 17, 2.5, and 0.75 s^{-1}, respectively, which are in reasonably good agreement with the values measured in Fig. 3*A*.

electron transfer to occur. We have thus concentrated our attention on the second electron [$k_{AB}(2)$] and proton [$k_{H^+}(2)$] transfer rates that are critically dependent on protonation events. The pH dependencies of $k_{AB}(2)$ and $k_{H^+}(2)$ are presented in Fig. 3 *A* and *B*, respectively. As seen previously in *Rb. sphaeroides* (6), the kinetics of the second electron transfer from Q_A^- to Q_B^- are biphasic. For simplicity in comparing the $k_{AB}(2)$ curves from the different strains, we have plotted only the major component.

In the wild type, $k_{AB}(2)$ decreases continuously from low to high pH. At pH 4.5, this rate is $1.7 \times 10^4\ s^{-1}$, decreasing to $2 \times 10^3\ s^{-1}$ at pH 8. In RCs from the double mutant, $k_{AB}(2)$ is substantially decreased compared to the wild type. At pH 8, $k_{AB}(2)$ is ≈4 orders of magnitude smaller than in the wild type—i.e., $k_{AB}(2) \approx 0.2\ s^{-1}$. This value is consistent with the cytochrome oxidation measurements (Fig. 2), which show that for flash repetition frequencies smaller than 0.2 Hz, the $\Delta A_3/\Delta A_1$ ratio becomes close to 1. The apparent pK (≈5) displayed in the $k_{AB}(2)$ curve for the double mutant is much lower than in the wild type (≈8).

As observed in Fig. 3*A*, the compensatory mutations present in the RCs from the class 3 and class 4 strains substantially increase (at pH 8, ≈25-fold and ≈10-fold, respectively) the second electron transfer rates compared to the PS⁻ double mutant. However, the $k_{AB}(2)$ values measured in RCs of both suppressor strains are still much smaller than that of the wild type. At pH 8, $k_{AB}(2) \approx 2\ s^{-1}$ in the class 4 strain and $\approx 5\ s^{-1}$ in the class 3 strain. The ratios between the $k_{AB}(2)$ values measured in the wild type and in both suppressor strains increase with pH, due to the steeper slopes of the $k_{AB}(2)$ curves for class 4 RCs (−0.9 H^+/e^-) and class 3 RCs (−0.75 H^+/e^-) compared to that of the wild type (−0.6 H^+/e^-).

The rate constants for transfer of the second proton to Q_B have been measured in the range pH 6–9 by dye absorbance changes. These data are presented in Fig. 3*B*. As for k_{AB} (2), the kinetics of proton donation are biphasic, and we have shown only the major component. The main observation that can be derived from these measurements is that the rates of the second proton donation to Q_B roughly match those of the second electron transfer. The values of $k_{AB}(2)$ and $k_{H^+}(2)$ are clearly similar to each other for the RCs of both the class 3 and class 4 strains. The exception is the double-mutant strain, for which $k_{H^+}(2)$ is higher than $k_{AB}(2)$ above pH 7. However, it is illogical that electron transfer could be delayed by ≈5 s [at pH 8: $k_{AB}(2) = 0.2\ s^{-1}$; $k_{H^+}(2) = 1$–$2\ s^{-1}$] after a proton has been transferred to Q_B. Because of the very slow $Q_A^- \rightarrow Q_B^-$ electron transfer process in this mutant, it is likely that part of the proton uptake kinetics at the second flash is due to rapid proton uptake by proteic groups in response to the formation of Q_A^-. We have verified this hypothesis by measuring the kinetics of proton uptake in the Q_A^- state in the presence of an inhibitor of the Q_A to Q_B electron transfer. These kinetics are very fast (data not shown). The $k_{H^+}(2)$ values measured in the double mutant above pH ≈7 are therefore probably increased by some contribution of proton uptake by Q_A^-.

The temperature dependencies of $k_{AB}(2)$ were measured in the four types of RCs. The Eyring plots are presented in Fig. 4 and the derived activation parameters are in Table 1. RCs of the wild-type, double-mutant, and class 3 strains display about the same activation energy [$\Delta H^{\ddagger}(2)$]: 2.38 ± 0.12, 2.20 ± 0.24, and 1.89 ± 0.12 kcal/mol (1 cal = 4.184 J), respectively. However, RCs of the class 4 strain display a $\Delta H^{\ddagger}(2)$ value for the second electron transfer process that is 3 times higher: 8.18 ± 0.48 kcal/mol. As a consequence, second electron transfer rates in the two suppressor strains are more similar at 28°C (where the cells are grown under photosynthetic conditions) than at 21°C. A substantial increase in the activation free energy of the $Q_A^- \rightarrow Q_B^-$ electron transfer process, $\Delta G^{\ddagger}(2)$, is observed in the double mutant (16.85 ± 0.60 kcal/mol; T = 293 K) compared to the wild type (12.30 ± 0.50 kcal/mol; T = 293 K), but both types of suppressor mutations reduce this value to nearly the same extent: 15.08 ± 0.50 and 15.50 ± 0.50 in class 3 and class 4 RCs, respectively (T = 293 K).

Electrostatic Influence of the Mutations on the Energetics of the Quinone System. The influence of the mutations on the free energy gap (ΔG^0) between the $P^+Q_A^-$ and $P^+Q_B^-$ states was studied by measuring the $Q_A^-Q_B \leftrightarrow Q_AQ_B^-$ equilibrium constant value, K_2, in the different strains. This was achieved by measuring the pH dependence of the rate constants of the $P^+Q_A^-$ (k_{AP}) and $P^+Q_B^-$ (k_{BP}) charge recombination processes. K_2 was then estimated by applying the formula derived by Wraight (19): $1+K_2 = k_{AP}/k_{BP}$. ΔG^0 is calculated from K_2 as

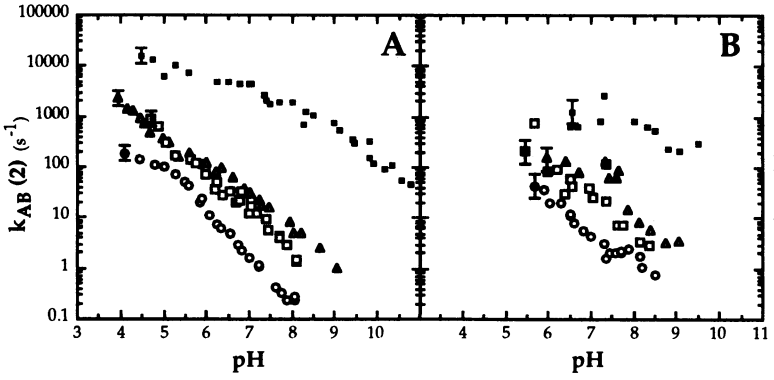

FIG. 3. pH dependencies of the rate constants of the second electron [$k_{AB}(2)$] (*A*) and second proton [$k_{H^+}(2)$] (*B*) transfers in the RCs (≈1 μM) from the wild type (■), the Ala-L212/Ala-L213 double mutant (○), and the class 3 (Ala-L212/Ala-L213/Leu-M231 (△), and class 4 (Ala-L212/Ala-L213/Asp-M43) (□) suppressor strains. (*A*) Conditions were 40 μM cytochrome *c*, 1 mM ascorbic acid, 100 μM coenzyme Q_6, and 0.03% Triton X-100. Buffers were Mes, Mopso, and Tris depending on the pH. (*B*) Conditions were 100 μM coenzyme Q_6, 100 μM ferrocene, and 40 μM dyes (cresol red, phenol red, bromocresol purple, and/or chlorophenol red, depending on pH). λ = 557 nm for phenol red and 582 nm for other dyes.

Table 1. Activation parameters for the second electron transfer reaction

Strain	$\Delta H^{\ddagger}(2)$, kcal/mol	$\Delta S^{\ddagger}(2)$, kcal·mol^{-1}·K^{-1}	$\Delta G^{\ddagger}(2)$ (kcal/mol)	$\Delta G^{\ddagger}(2)$ meV
Wild type	2.38 ± 0.12	−0.033 ± 0.002	12.30 ± 0.50	533 ± 25
Double mutant	2.20 ± 0.24	−0.050 ± 0.002	16.85 ± 0.60	733 ± 30
Class 3 suppressor	1.89 ± 0.12	−0.045 ± 0.002	15.08 ± 0.50	657 ± 25
Class 4 suppressor	8.18 ± 0.48	−0.025 ± 0.002	15.50 ± 0.50	677 ± 25

Activation parameters for the second electron transfer reaction in RCs from the wild type, the double mutant, and the class 3 and class 4 suppressor strains. For mutations carried by these strains, see text. Conditions were pH 7, 100 mM NaCl, and T = 293 K. These values are deduced by fitting the data of Fig. 4 by the Eyring equation: $k_{AB}(2) = k_B T/h \times \exp[(\Delta S^{\ddagger}/R) - (\Delta H^{\ddagger}/RT)]$.

$\Delta G^0 = -RT\ln K_2$. Since little difference (<5%) was observed between the k_{AP} values measured in the suppressor strains and the double mutant compared to the wild type (data not shown), we have used the value of k_{AP} determined for the wild type in ref. 15 in the calculations of ΔG^0 for all of the strains (Fig. 5). As we have previously pointed out (15), the sharp variations of ΔG^0 observed at low and high pH in the wild type *Rb. capsulatus* could reflect, in part, the ionization of Asp-L213 and Glu-L212, respectively, similarly to what has been suggested for *Rb. sphaeroides* (5–9). Consideration of these ΔG^0 values at pH 8, where Asp-L213 (but probably not Glu-L212) is ionized in the wild type, allows us to evaluate the change in the coulombic interaction energy between Q_B^- and its environment due to the different mutations. In the double mutant at pH 8, Q_B^- appears to be stabilized by ≈60 meV compared to the wild type. This value could be slightly underestimated because, in this mutant, $P^+Q_B^-$ may decay through the direct route to the ground state by an electron tunneling effect (10) rather than through Q_A by a thermally activated process. The substantial stabilization of Q_B^- in the double mutant may be understood in terms of the absence of ionized Asp-L213; Glu-L212 should still be protonated at this pH in the wild type (6, 8).

In the suppressor strains, Q_B^- is predictably destabilized compared to the double mutant, due to the loss of a positive charge in the class 3 strain (Arg-M231 → Leu) or to the addition of a negative charge in the class 4 strain (Asn-M43 → Asp, assuming that the pK of Asp-M43 is much lower than 8). In the class 3 strain at pH 8, ΔG^0 is reduced by at least 30 meV compared to the double mutant, whereas it is reduced by at least 20 meV in the class 4 strain.

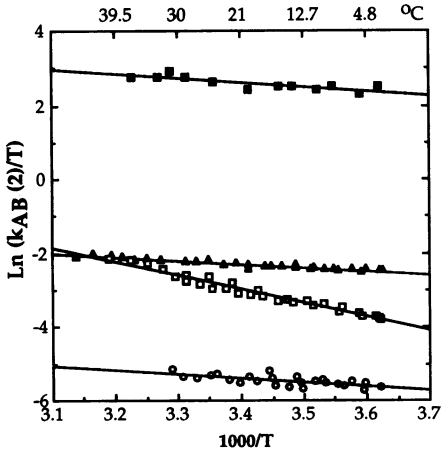

FIG. 4. Eyring plots of rate constants for the $P^+Q_A^-Q_B^- \rightarrow P^+Q_AQ_B^{2-}$ in RCs from the wild type (■), the Ala-L212/Ala-L213 double mutant (○), and the class 3 (Ala-L212/Ala-L213/Leu-M231) (△) and class 4 (Ala-L212/Ala-L213/Asp-M43) (□) suppressor strains. Slopes of lines (drawn by linear regression) lead to $\Delta H^{\ddagger}$ values of 0.12 ± 0.01 eV for the wild type, 0.114 ± 0.010 eV for the double mutant, 0.102 ± 0.010 eV for the class 3 suppressor strain, and 0.335 ± 0.015 eV for the class 4 suppressor strain. Conditions are as in Fig. 3*A* at pH 7.

DISCUSSION

In this paper, we evaluate the different energetic and kinetic properties of electron and proton transfer in RCs from three strains that have identical amino acid sequences in the Q_B binding site. All of these strains lack two acidic residues, Glu-L212 and Asp-L213, that have been shown to be components of the proton transfer pathway to reduced Q_B in the wild type (5, 6, 8, 12). These strains are the photosynthetically incompetent site-specific double-mutant Glu-L212/Asp-L213 → Ala-L212/Ala-L213, and two photocompetent derivatives that carry intergenic suppressor mutations located well outside of the Q_B binding pocket (class 3 strain, Glu-L212/Asp-L213/Arg-M231 → Ala-L212/Ala-L213/Leu-M231; class 4 strain, Glu-L212/Asp-L213/Asn-M43 → Ala-L212/Ala-L213/Asp-M43). This analysis reveals severe impairment of RC function in the double mutant and, more surprisingly, shows that both types of suppressor strains recover those functional, kinetic, and electrostatic properties to a similar extent.

Semiquinone oscillations are absent in the double mutant at pH 7.8, but both suppressor strains exhibit these oscilla-

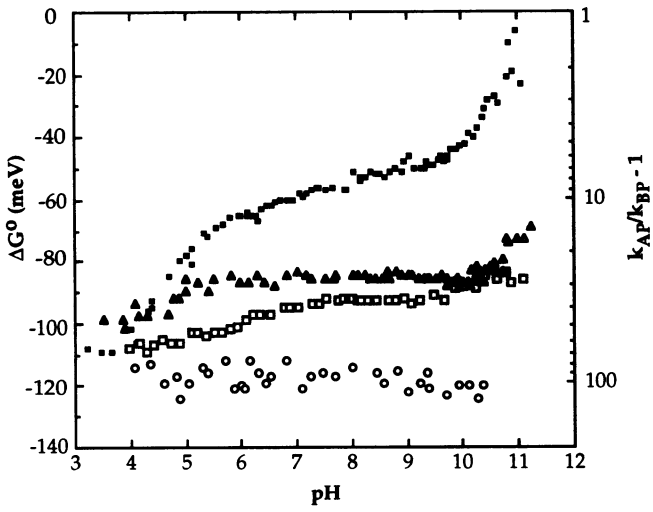

FIG. 5. pH dependence of the free energy gap, ΔG^0, between the $P^+Q_A^-$ and $P^+Q_B^-$ states in the RCs (≈1 μM) from the wild type (■) *Rb. capsulatus* and the class 3 (Ala-L212/Ala-L213/Leu-M231) (△) and class 4 (Ala-L212/Ala-L213/Asp-M43) (□) suppressor strains. These ΔG^0 values were derived from independent measurements of k_{AP} and k_{BP}, by $\Delta G^0 = -RT\ln(k_{AP}/k_{BP} - 1)$ (15). Data points for the Ala-L212/Ala-L213 double mutant (○) strictly refer to the right axis. The very slow $P^+Q_B^-$ decay observed in this mutant suggests a direct route (not through Q_A) for the charge recombination process (see text). Therefore, in the double mutant, the ΔG^0 values calculated from the above expression may underestimate the stabilization energy and may distort its pH dependence.

tions, accounting for the recovery of the photosynthetic phenotype in these strains. However, under favorable conditions the double mutant RCs show the ability to function as well as the suppressor strains do at pH 8. This is the case for semiquinone oscillations at pH 6.2, for cytochrome oxidation turnover at low flash repetition frequency at pH 8, and in the presence of sodium azide. Clearly, these improvements in the function of the double mutant under the above conditions can be understood in terms of the extremely slow electron and proton transfer processes to Q_B at physiological pH. This was readily verified by direct measurements of these rates. At pH 8, $k_{AB}(2)$ is found to be almost 4 orders of magnitude smaller than the wild-type value.

Much to our surprise, although the rates of second electron and proton transfer in the RCs of the suppressor strains are increased 10–25 times compared to the double mutant, they are still >2 orders of magnitude smaller than those of the wild type. The similar growth rates of these strains and of the wild type under photosynthetic conditions (14) suggest that these low electron and proton transfer rates are still above the threshold limits for photosynthetic function. It is also possible that *in vivo*, in the energized membrane, electron transfer rates in the RC are faster than those displayed in the isolated state.

It is most striking that the electron and proton transfer kinetic parameters in the two suppressor strains are restored to the same levels. This suggests that an analogous physical mechanism for phenotypic suppression is induced by these two types of compensatory mutations, Arg-M231 → Leu (class 3) and Asn-M43 → Asp (class 4), which are situated in very different parts of the protein. The simultaneous acceleration of second electron and proton transfers in the suppressor strains is difficult to understand without the activation of optional proton transfer pathways. These may involve water molecules (10–12) and would be less active in the double mutant for electrostatic reasons. The recovery of a more negative Q_B environment, restored by either type of suppressor mutation, allows these pathways to be activated. The proton transfer pathways that operate in the suppressor strains may already exist in the wild type but may not be used because another is more efficient.

In the class 4 strain, the activation energy for the second electron transfer process was found to be 3 times as high as in the other three strains. This suggests a special activation energy barrier for proton transfer in this strain, possibly involving a breathing motion of the protein at the L–M–H interface. In the double mutant, the lack of protonatable residues at positions L212 and L213 causes an elevated free energy barrier for activation of the second electron (and proton) transfer. Interestingly, the free energy barrier is similarly reduced in both suppressor strains.

The overall electrostatic environments of Q_B^- in the class 3 and class 4 RCs are quite similar at neutral pH, as seen in the pH dependence of ΔG^0. However, the extent of Q_B^- stabilization is slightly smaller in the class 3 strain. This difference cannot be explained by the distance of the M43 and M231 residues from Q_B (9 and 15 Å, respectively); therefore, it might be due to different electrostatic screening in the two types of RCs. A difference in solvation energy of Q_B^- in both strains, due to electrostatic and/or structural changes, cannot be ruled out. The pH dependence of ΔG^0 in the class 4 strain is reminiscent of those of the class 3 strain and the wild type. However, the variations observed at low and high pH for the class 4 strain are attenuated in comparison to the class 3 strain, consistent with the possible higher screening effect in the former strain. These similar patterns suggest that Glu-L212 and Asp-L213 may not be the unique groups involved in the pH dependence of ΔG^0 in the RCs at high and low pH, respectively, but may participate in a larger network of interacting amino acids.

Conclusions. The most remarkable finding is that both types of distant mutations that compensate for the loss of Glu-L212 and Asp-L213 restore to nearly the same extent the semiquinone oscillation patterns, electron and proton transfer kinetics, and the electrostatic environment of the secondary quinone. In addition, the RCs from the double mutant do not appear to have lost these functions completely but can show properties similar to those of the suppressor strains when the pH is decreased by 1.5 to 2 units. It is therefore likely that the important role of the compensatory mutations (at a distant site) is to enhance the negative environment in the vicinity of Q_B, thereby raising the apparent overall pK for efficient proton transfer to Q_B^{2-}. This threshold limit could define the difference in phenotype between the double-mutant and the suppressor strains. This accentuates the major electrostatic role of the protein in tuning pKs of the groups involved in proton delivery. Even if the single additional mutations present in the suppressor strains do not fully restore the wild-type proton transfer kinetics, they ensure by long-range electrostatic effects sufficient recovery for the cells to grow with nearly the same rates as the wild type. The absence of Asp-L213 and Glu-L212 in these strains emphasizes that they are not essential for RC function and probably highlights the role of water molecules in many potential pathways for proton conduction within RCs and in other proton translocating membrane proteins as well.

We thank Dr. F. Reiss-Husson for helpful discussions, and Drs. F. Stevens and D. Tiede for critical reading of the manuscript. M. C. Gonnet is thanked for technical assistance in growing the cells of the different strains. This work was supported by North Atlantic Treaty Organization (CRG. 920725) and National Science Foundation–Centre National de la Recherche Scientifique (CDP 900350) grants and by the U.S. Department of Energy, Office of Health and Environmental Research under Contract W-31-109-ENG-38 (D.K.H. and M.S.). P.M. was supported by the French Ministère des Affaires Etrangères, by European Community (PECO fellowship) and OTKA (1978/1991). M.S. was also supported by Public Health Service Grant GM36598.

1. Deisenhofer, J., Epp, O., Miki, R., Huber, R. & Michel, H. (1985) *Nature (London)* **318**, 618–624.
2. Feher, G., Allen, J. P., Okamura, M. Y. & Rees, D. C. (1989) *Nature (London)* **339**, 111–116.
3. Chang, C.-H., El-Kabbani, O., Tiede, D., Norris, J. & Schiffer, M. (1991) *Biochemistry* **30**, 5352–5360.
4. Ermler, U., Fritzsch, G., Buchanan, S. & Michel, H. (1992) in *Research in Photosynthesis*, ed. Murata, N. (Kluwer, Dordrecht, The Netherlands), Vol. 1, pp. 341–347.
5. Takahashi, E. & Wraight, C. A. (1990) *Biochim. Biophys. Acta* **1020**, 107–111.
6. Takahashi, E. & Wraight, C. A. (1992) *Biochemistry* **31**, 855–866.
7. Paddock, M. L., McPherson, P. H., Feher, G. & Okamura, M. Y. (1990) *Proc. Natl. Acad. Sci. USA* **87**, 6803–6807.
8. Paddock, M. L., Rongey, S. H., Feher, G. & Okamura, M. Y. (1989) *Proc. Natl. Acad. Sci. USA* **86**, 6602–6606.
9. Shinkarev, A., Takahashi, E. & Wraight, C. A. (1993) *Biochim. Biophys. Acta* **1142**, 214–216.
10. Hanson, D. K., Baciou, L., Tiede, D. M., Nance, S. L., Schiffer, M. & Sebban, P. (1992) *Biochim. Biophys. Acta* **1102**, 260–265.
11. Beroza, P., Fredkin, D. R., Okamura, M. Y. & Feher, G. (1992) in *The Photosynthetic Bacterial Reaction Center II: Structure, Spectroscopy, and Dynamics*, NATO ASI Series, eds. Breton, J. & Vermeglio, A. (Plenum, London), pp. 363–374.
12. Rongey, S. H., Paddock, M. L., Feher, G. & Okamura, M. Y. (1993) *Proc. Natl. Acad. Sci. USA* **90**, 1325–1329.
13. Hanson, D. K., Tiede, D. M., Nance, S. L., Chang, C.-H. & Schiffer, M. (1993) *Proc. Natl. Acad. Sci. USA* **90**, 8929–8933.
14. Hanson, D. K., Nance, S. L. & Schiffer, M. (1992) *Photosynth. Res.* **32**, 147–153.
15. Baciou, L., Bylina, E. J. & Sebban, P. (1993) *Biophys. J.* **65**, 652–660.
16. Wraight, C. A. (1977) *Biochim. Biophys. Acta* **459**, 525–531.
17. Vermeglio, A. (1977) *Biochim. Biophys. Acta* **459**, 516–524.
18. Takahashi, E. & Wraight, C. A. (1991) *FEBS Lett.* **283**, 140–144.
19. Wraight, C. A. (1981) *Isr. J. Chem.* **21**, 348–356.